Tellus SERIES B CHEMICAL AND PHYSICAL METEOROLOGY
PUBLISHED BY THE INTERNATIONAL METEOROLOGICAL INSTITUTE IN STOCKHOLM

Black carbon aerosols over the Himalayas: direct and surface albedo forcing

By VIJAYAKUMAR S. NAIR[1]*, S. SURESH BABU[1], K. KRISHNA MOORTHY[1], ARUN KUMAR SHARMA[2], ANGELA MARINONI[3,4] and AJAI[2], [1]*Space Physics Laboratory, Vikram Sarabhai Space Centre, Thiruvananthapuram, India;* [2]*Space Applications Centre, Ahmedabad, India;* [3]*CNR-ISAC-Institute of Atmospheric Sciences and Climate, Bologna, Italy;* [4]*EV-K2-CNR Committee, Bergamo, Italy*

(Manuscript received 19 September 2012; in final form 5 August 2013)

ABSTRACT

Absorbing aerosols such as black carbon (BC) or dust over high-altitude Himalayan regions have potential implications on the regional climate and hydrological cycle over South Asia. Making use of extensive measurements of atmospheric BC from several Himalayan stations, an assessment of radiative forcing due to direct and snow-albedo darkening is examined. Generally, BC concentration in the atmosphere peaks during pre-monsoon season over the Himalayas and the climatological mean of atmospheric BC over Hanle (western Himalayas, 4.5 km msl) and Nepal Climate Observatory-Pyramid (central Himalayas, 5 km msl) are 106 ± 27 ng m^{-3} and 190 ± 95 ng m^{-3}, respectively. Based on the optical and physical properties of composite aerosols measured at Hanle, clear sky direct radiative forcing (DRF) at the top of the atmosphere is estimated as 1.69 W m^{-2} over snow surface and -1.54 W m^{-2} over sandy surface during pre-monsoon season. The estimated amount of BC in the snow varied from 117 to 1.7 μg kg^{-1} for wide range of dry deposition velocities (0.01–0.054 cm s^{-1}) of BC, snow depth (2–10 cm) and snow densities (195–512 kg m^{-3}). Using a size-resolved wet scavenging parametrisation, the amount of BC on snow due to wet scavenging is estimated as 29 μg kg^{-1} for an accumulated snow depth of 27 cm. For the range of 10–200 μg kg^{-1} of BC in snow, the diurnally averaged forcing due to snow darkening has been found to vary from 0.87 to 10.2 W m^{-2} for fresh snow and from 2.6 to 28.1 W m^{-2} for the aged snow, which is significantly higher than the DRF. The direct and surface albedo radiative forcing could lead to significant warming over the Himalayas during pre-monsoon.

Keywords: black carbon, Himalayan aerosols, snow albedo, radiative forcing

1. Introduction

Black carbon (BC) aerosols are known for their potential to perturb the radiative balance of the Earth–Atmosphere system and thus forcing the regional climate in numerous pathways (Lau et al., 2006; IPCC, 2007; Ramanathan and Carmichael, 2008; Flanner et al., 2009) leading to complex responses in the Earth–Climate system (Hansen et al., 1997; Shindell et al., 2010). In addition to the direct radiative interaction with solar and terrestrial radiation via scattering and absorption, BC aerosols modify the cloud microphysical properties (indirect and semi-direct effect) and reduce the albedo of the snow due to BC deposition (Warren and Wiscombe, 1980; Flanner et al., 2007; IPCC, 2007). The radiative forcings due to direct, semi-direct and snow-albedo effects of BC aerosols and their implications on the hydro-climate are amongst the major challenges in the regional climate impact assessments (Flanner et al., 2007; Menon et al., 2010; Nigam and Bollasina, 2010).

Deposition of absorbing aerosols (mainly BC and dust) on highly reflecting surfaces (like snow or ice) would reduce the surface albedo significantly and result in positive radiative forcing (warming) at the top of the atmosphere (TOA) (Hansen and Nazarenko, 2004; Jacobson, 2004; Painter et al., 2007; Flanner et al., 2009). The global mean radiative forcing due to BC-induced snow darkening is estimated as $+0.1 \pm 0.1$ W m^{-2}, which offsets $\sim$20% of the cooling due to aerosols at the TOA (IPCC, 2007). Hansen et al. (2005) have shown that snow-albedo modification via BC deposition has very high efficacy of climate forcing compared to direct and semi-direct BC forcings and that for most of the

*Corresponding author.
email: vijayakumarsnair@gmail.com

Citation: Tellus B 2013, **65**, 19738, http://dx.doi.org/10.3402/tellusb.v65i0.19738

other climate forcing agents. Even though several studies have addressed the radiative impacts of BC on snow, quantitative estimates of radiative forcings have been made only recently (Hansen and Nazarenko, 2004; Flanner et al., 2009).

The great Himalayas have profound significance, with its glaciers believed to be the largest fresh water reservoirs outside the polar region, in the hydrological cycle via thermal and dynamical influence on the large-scale flow patterns associated with summer monsoon over South Asia (Hahn and Manabe, 1975; Vaux et al., 2012). The day-to-day lives of millions of people, their agricultural practices and their economy are directly or indirectly controlled by the monsoon rainfall and the river discharges fed by the Himalayan glaciers (Vaux et al., 2012). Even though there are several geological and glaciological reasons for the retreat or advance of glaciers over the Himalayas (Bolch et al., 2012), surface darkening due to BC deposition is being increasingly projected by modelling studies as a major factor contributing to the faster snow melting (Flanner et al., 2009; Menon et al., 2010; Qian et al., 2011) and several caveats have been put forward. Recently, BC-induced free-tropospheric heating (elevated heat pump) (Lau et al., 2006) and snow-albedo reduction due to BC deposition over the Himalayan region (Qian et al., 2011) has received significant scientific attention because of its projected implications on the regional climate, monsoon and hydrological cycle (Nigam and Bollasina, 2010).

Generally, climate model simulations of BC-induced snow darkening have revealed significant consequences on regional climate and hydrological cycles during the pre-monsoon season (Menon et al., 2010; Qian et al., 2011). However, it is very difficult to simulate the aerosol fields over complex and high terrain and most of the climate models simulate very low BC concentration in the atmosphere over south Asia especially over the Indian region (Ganguly et al., 2009; Menon et al., 2010; Nair et al., 2012). Even though aerosol BC over the Himalayas, in general, and glaciers in particular, have been a topic of prime scientific interest, there are not much measurements of BC over the western and southern slopes of the Himalayas, while measurements of BC on snow have been reported from several locations on the Tibetan plateau and south-eastern Himalayas (Ming et al., 2008, 2009; Xu et al., 2009; Huang et al., 2011). In the backdrop of all of the above, continuous measurements of aerosols including BC have been initiated at high-altitude stations as well as lower Himalayan stations under the Aerosol Radiative Forcing over India (ARFI) project of ISRO-Geosphere Biosphere Programme (I-GBP). In this article, radiative implications of BC aerosols via direct radiative forcing (DRF) and snow-albedo forcing over the southern and western Himalayan region are discussed based on a measurement-cum-modelling approach.

2. Experimental details and data

The major objective of ARFI project under the I-GBP is to build and maintain a network of systematic observations of aerosol parameters relevant for the climate change studies over the Indian region. Currently, there are 35 stations operational under this project and various aerosol parameters are being measured based on the common protocol (Moorthy et al., 2013). Long-term measurements as well as field campaigns are being carried out under the umbrella of ARFI project to investigate the climatic implications of BC aerosols over the Himalayan region. The continuous measurements of near-surface BC mass concentrations carried out at high-altitude western trans-Himalayan station, Hanle (32.78°N, 78.96°E, ~4520 m), and three lower Himalayan stations [Nainital (29.4°N, 79.5°E, 1958 m), Kullu (31.9°N, 77.1°E, 1154 m) and Dehradun (30.34°N, 78.04°E, 700 m)] using inter-compared Aethalometers formed the primary database for this study. In addition, a recent field expedition was conducted to Satopanth glaciers (30.76°N, 79.4°E, 4388 m) from 28 September 2011 to 5 October 2011 during which measurements of BC in the atmosphere were made at various locations en route for the first time. These observations were compared with BC concentrations measured at the Nepal Climate Observatory-Pyramid (NCO-P, 27.95°N, 86.82°E, 5079 m), using a Multi-Angle Absorption Photometer (MAAP), under SHARE, Ev-K2 CNR project (Bonasoni et al., 2010). The specifications of measurement locations and period of BC measurements used in this study are given in Table 1. The entire data are synthesised to obtain a spatio-temporal distribution of atmospheric BC over the southern slopes of the Himalayas. Figure 1 shows the location of measurement sites mentioned above on the background of the topographic image.

To understand the characteristics of BC aerosols near/over the glaciers, a scouting experiment has been carried out to Satopanth glaciers (~4400 m) shown in Fig. 1.

Table 1. The details of measurement locations and period of measurements

Station name	Region	Altitude (km)	Data period
Hanle	Western Himalayas	4.5	08/2009 to 12/2011
Nainital	Lower Himalayas	1.9	01/2005 to 08/2012
Kullu	Lower Himalayas	1.2	07/2009 to 03/2012
Dehradun	Lower Himalayas	0.7	03/2007 to 08/2010
Satopanth glacier*	Western Himalayas	4.4	09/2011 to 10/2011
NCO-P	Central Himalayas	5.1	03/2006 to 02/2008

*Measurements made during scientific expedition to Satopanth glacier.

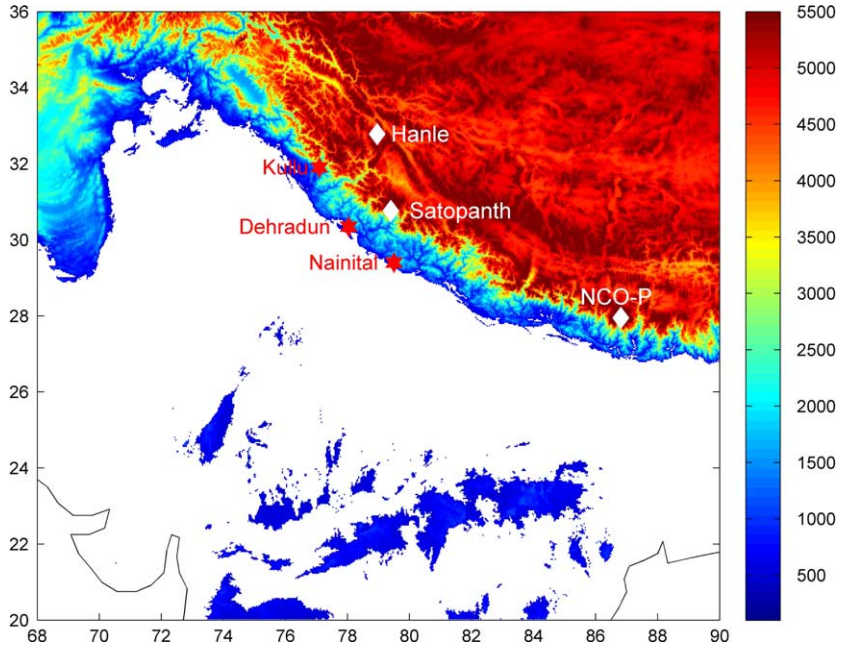

Fig. 1. Measurement locations over the Himalayas are superposed over the terrain height map (Topography from US Geological Survey's EROS data centre). Measurement sites include (i) Nainital, Dehradun and Kullu (lower Himalayan stations), (ii) Hanle and NCO-P (high-altitude stations) and (iii) Satopanth (campaign location near Satopanth glaciers).

The expedition started on 28 September 2011 from Badrinath and reached near Satopanth Lake on 2 October 2011 and returned to Badrinath on 5 October 2011. The measurements of atmospheric BC were made en route and also at the glacier site using a portable Aethalometer (model AE-41), which was inter-compared with the similar instruments prior to the campaign. Due to power limitations, BC measurements were restricted to 2–3 hours (on average) at noon, when the thermal convections are strong locally. As a measurement protocol, BC measurements were made mostly on the peak of the nearest mountain en route. Measurements were always made far away and in the upwind areas of the night camp location. The meteorological conditions that prevailed during the expedition include: (1) partially cloudy sky condition mostly due to orographic clouds, (2) snowfall events on 1 and 2 October, 2011, and (3) moderate wind speed condition, which was mostly coming from the valley region.

The continuous measurements of BC mass concentrations in the atmosphere are being made from Hanle (Babu et al., 2011) and lower Himalayan stations (Pant et al., 2006). The aerosol observatory at Hanle is located atop Mt. Saraswathi, far away from local sources and pollution, and is being operated since 2009. The other high-altitude station, NCO-P, in the Eastern Himalayas, is located in the high Khumbu Valley, not far from the Mt. Everest base camp. The lower Himalayan stations are relatively more populated and impacted by local sources. Nainital is located above the mean boundary layer height of the valley region and data collected from this station are extensively used for understanding the vertical transport of aerosols due to large-scale convection (Pant et al., 2006). Kullu and Dehradun are relatively more close to the local sources and are known tourist hotspots of the area. Both Kullu and Nainital have glacier proximity also.

All of the atmospheric BC measurements have been made using multi-wavelength Aethalometer (Magee Scientific, USA) working on the principle of optical attenuation technique (Hansen et al., 1984), except for NCO-P observations. The principle of operation, data deduction and error handling of Aethalometer have been extensively discussed in several papers (Arnott et al., 2005; Nair et al., 2007), hence not repeated here. In the present setup, the instrument was operated continuously at a flow rate of 5 LPM with data recorded at 5-minute intervals. The inherent uncertainties associated with the loading and multiple scattering effects of aerosols on the filter tape in Aethalometer measurements can contribute upto $\sim$20% as described by Arnott et al. (2005) and Nair et al., (2007, 2008). Based on the extensive inter-comparison of instruments used for measuring aerosol absorption, Müller et al. (2011) have shown that, in general, Aethalometer measurements are in good agreement with photo-acoustic and other filter-based instruments such as Particle Soot Absorption Photometers (PASP) and MAAP. At NCO-P, the measurement of the aerosol absorption coefficient was obtained by MAAP that measures the

transmission and the backscattering of a light beam (Petzold and Schonlinner, 2004) incident on a fibre filter, where aerosol particles are deposited by sampling flow. It was operated at 16 LPM and 30-minute integration time.

3. Results and discussions

3.1. BC over the Himalayas

3.1.1. Expedition to Satopanth glaciers. A pilot expedition was undertaken to the Satopanth glaciers from 28 September to 5 October 2011, where atmospheric BC measurements were made over the de-glaciated valley of Satopanth glacier as well as close to the regions where fresh snowfall occurs. Snowfall events were observed during 1–2 October close to the measurement site. The spatial pattern of the mean BC values measured on each day of the expedition is shown in Fig. 2. High concentrations are observed near to the Badrinath (Mana village from where the expedition started) due to the relatively higher human activities around the valley regions in association with the pilgrim season. Subsequently, as we moved away and to higher altitudes, the magnitude of BC in the atmosphere decreased significantly and we have observed almost a steady BC value of 190 ng m^{-3} at the remote Himalayan regions. BC exhibited large temporal variabilities at the lower altitudes and close to the inhabited areas due to the proximity to the time-dependent source activities and diurnal evolution of the boundary layer (Nair et al., 2007). It is known that the atmospheric BC over the Himalayas shows significant temporal variations in association with meso scale and synoptic scale changes in advection pattern (Bonasoni et al., 2010; Marinoni et al., 2010; Babu et al., 2011). The measurements were limited to a few days over the Satopanth, hence the seasonal evolution and sources of BC aerosols over the Satopanth glaciers are rather unclear. As such, we have analysed the continuous measurements reported by Babu et al. (2011) at Hanle and Marinoni et al. (2010) at NCO-P for seasonal variations of atmospheric BC over high Himalayas.

3.1.2. Measurements from Hanle and NCO-P. Figure 3 shows the monthly mean climatological variations of atmospheric BC at NCO-P and Hanle (Marinoni et al., 2010; Babu et al., 2011). Despite the Hanle values being significantly lower than those at NCO-P throughout the year, in general, similar seasonal variations are observed at both the locations with high values during pre-monsoon season (March–May) and low during summer (June–September). The higher BC at the NCO-P could be attributed to the confinement of aerosols over the Khumbu valley and/or due to the significant long-range transport from the major source regions (Bonasoni et al., 2010; Marinoni et al., 2010). Moreover, the deep Himalayan valleys can be efficient and persistent channels for transporting large amounts of particles to the high altitudes during daytime through the up-valley breeze, as shown by analysis of diurnal variation and correlation with meteorological parameters in Marinoni et al. (2010). In general, airmass back-trajectories reaching at NCO-P (central Himalayas) and Hanle (western Himalayas) mostly originated from West Asia (western most part of Asian sub-continent) during pre-monsoon

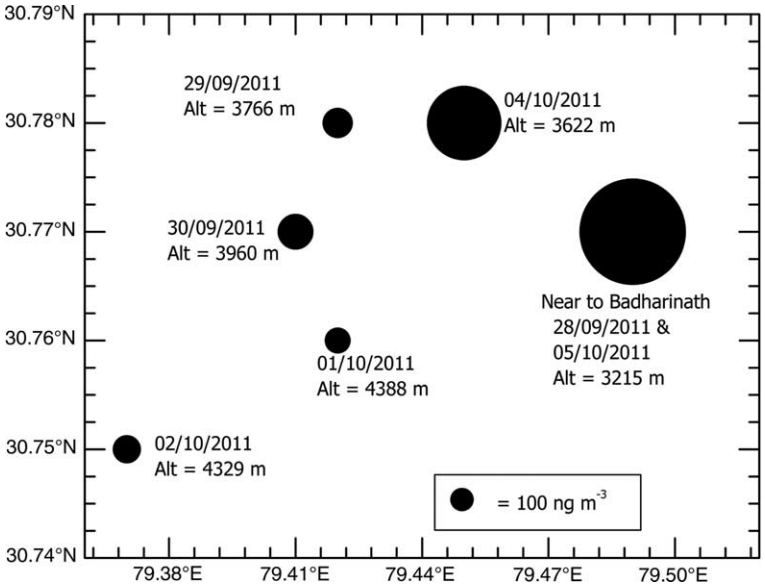

Fig. 2. Spatial pattern of atmospheric BC mass concentrations over the Satopanth region. Measurement date and altitude of observations are noted. The size of filled circles indicates the magnitude of the BC mass concentration.

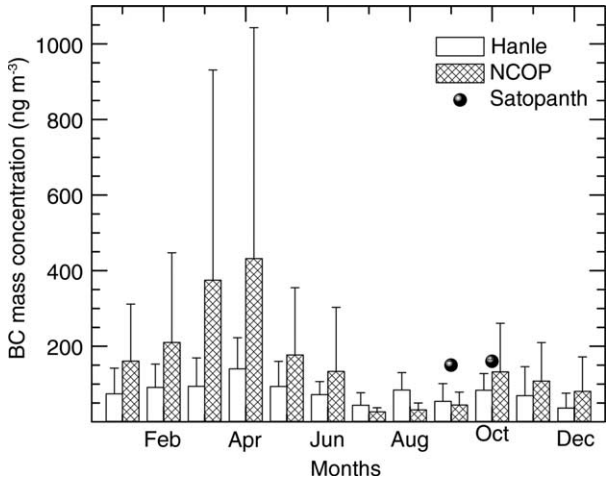

Fig. 3. Climatological monthly mean mass concentrations of atmospheric black carbon (BC) aerosols at Hanle and NCO-P. The vertical lines indicate the standard deviation of the data. The atmospheric BC values measured over Satopanth glacier is shown as filled circles.

season (Bonasoni et al., 2010; Babu et al., 2011). The mean value of atmospheric BC over Satopanth is much higher than the values reported from Hanle and NCO-P for the same season. This could partly be attributed to the pilgrim and tourist activities at Badrinath during the summer. As measurements from this region are limited only to this campaign, it is hard to draw definite conclusions based on these data. Notwithstanding this, the BC loads over the western and central Himalayas are high enough to potentially influence the radiation balance and hydrological cycle. Though information of BC on snow is available from several glaciers on the northeastern part of the Himalayas (Xu et al., 2009; Ming et al., 2010, 2012) and from Mt. Everest (Kaspari et al., 2011), the measurements of atmospheric BC concentrations over the Himalayas are limited (Marinoni et al., 2010; Babu et al., 2011), especially over the southern slopes. Simulation of BC in snow and its inter-comparison with measurements (e.g. Xu et al., 2009; Yasunari et al., 2010, 2013) and the climate implications were reported by several investigators (Flanner et al., 2009; Menon et al., 2010; Qian et al., 2011) using regional as well as global climate models.

3.1.3. BC from the lower Himalayan stations. Figure 4 shows the climatology of monthly mean BC in the atmosphere at the three lower Himalayan stations: Dehradun, Kullu and Nainital. In general, BC concentrations over these stations showed an increase with decrease in altitude, and larger (spatio-temporal) heterogeneity; with very high BC over Dehradun, and low values at Nainital with Kullu coming in-between. The seasonal variation of BC mass

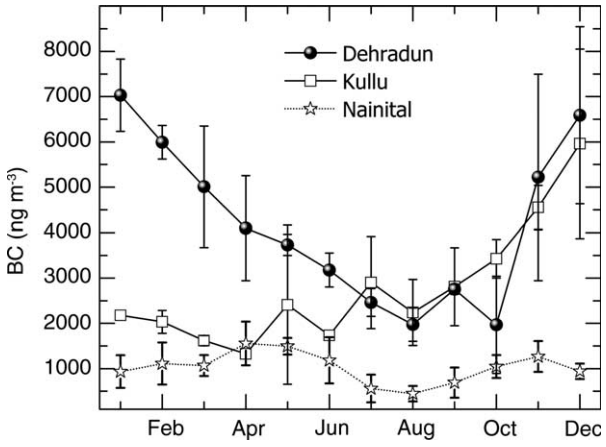

Fig. 4. Climatology of monthly variations of atmospheric BC mass concentrations at Dehradun, Kullu and Nainital.

concentration as a function of station altitude is shown in Fig. 5. All three stations in the lower Himalayas are tourist hotspots (from pre-monsoon through summer). Dehradun is at a lower altitude and is more inhabited than the other two locations. Nainital is located 1.9 km above the mean sea level (amsl) and far away from the local emissions and even above the local atmospheric boundary layer of the valley, except perhaps in summer. Seasonal variations of BC at Dehradun are quite similar to the seasonal variation of the BC over the plains, which shows wintertime "High" and

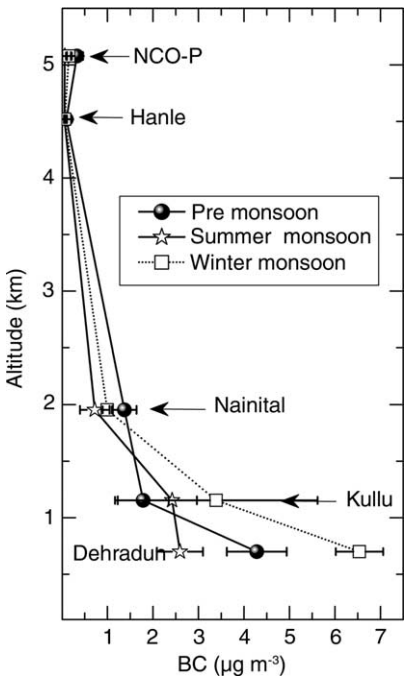

Fig. 5. Seasonal variation of atmospheric BC mass concentrations measured at Dehradun, Kullu, Nainital, Hanle and NCO-P as a function of station altitude.

summertime "low". The temporal variations are due to the contrasting wind patterns, boundary layer dynamics and precipitation associated with the Indian monsoon (Babu et al., 2004; Nair et al., 2007). In contrast to this, BC over Nainital shows a pattern which is closer to that of Hanle and NCO-P, with high values during pre-monsoon season in association with convective updrafts of BC from the valley as well as the advection from the West Asia and Indo-Gangetic Plain. Several investigations on the seasonal variation of atmospheric BC over the Himalayan regions using the back-trajectory analyses have revealed significant dependence on the origin and direction of airmass reaching the Himalayas (e.g. Babu et al., 2011). The transport pathways of aerosols over the Himalayas have been investigated by several authors (e.g. Bonasoni et al., 2010; Babu et al., 2011; Lu et al., 2012), though it is difficult to quantitatively assess the contribution of regional sources to the total aerosol loading. Using WRF-Chem and its adjoint analysis, Kopacz et al. (2011) have identified the significant contribution of BC from China, India and Nepal to five glaciers over the Himalayas and Tibetan plateau. Lu et al. (2012) have quantified the regional contribution of BC to the Himalayas and Tibetan Plateau from South Asia and East Asia as 67% and 17%, respectively, using an extensive back-trajectory analysis. Based on the inventory data and meteorological data, they have further shown that West Asia and Europe contribute significantly to the BC over the northern Himalayas, while Babu et al. (2011) have also shown West Africa and Europe impact at western-trans-Himalayas (Hanle) with very little transport from Indo-Gangetic Plain. The analysis of back-trajectories and background BC concentrations at NCO-P by Marinoni et al. (2010) showed that high BC levels are mainly associated with Middle East and Europe airmass origin, besides the regional circulation.

3.2. *BC deposition pathways*

3.2.1. Dry deposition. The snow darkening due to BC deposition has significant climate implications during pre-monsoon season because of favourable conditions such as: (1) high concentration of atmospheric BC (Marinoni et al., 2010; Babu et al., 2011); (2) intense solar radiation flux; and (3) decrease in snow cover and depth towards summer. The dry deposition of BC onto snow surface is estimated using hourly mean values of BC in the atmosphere for a dry deposition velocity of 0.01 cm s^{-1}, snow density of 195 kg m^{-3} and snow depth of 2 cm, as shown in Fig. 6. The amount of BC in the snow during the pre-monsoon period is estimated as 20.8 μg kg^{-1}. Furthermore, to get the range of BC values on snow, the dry deposition flux (μg m^{-2} s^{-1}) of BC aerosols to the snow surface has been estimated using the climatological mean BC mass concentration of 109 ± 26 ng m^{-3} as obtained from Hanle data. It should be noted that estimates of dry deposition velocity of BC and snow characteristics at or near Hanle are non-existing; so we have used dry deposition velocities ranging from 0.01 and 0.054 cm s^{-1} (Yasunari et al., 2013) and the snow density of 195 kg m^{-3} for fresh snow and 512 kg m^{-3} for aged snow based on Yasunari et al. (2010). The snow layer thickness is assumed to be 2 or 10 cm, since the dry deposition occurs on

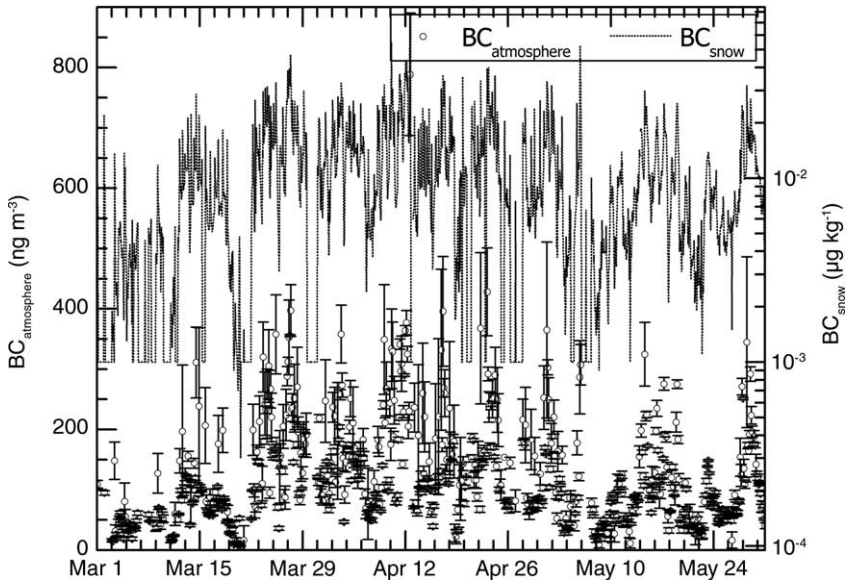

Fig. 6. Hourly mean values of BC (open circles) in the atmosphere and the estimated mass concentrations of BC in the top snow layer (dotted lines) due to dry deposition based on the dry deposition velocity used in Yasunari et al. (2010) over Hanle during pre-monsoon season, 2010.

the top layer of the snow. The amount of BC on snow over Hanle for the different dry deposition velocities and snow conditions varied from 1.7 to 117 μg kg^{-1} as shown in Table 2. The mean flux of BC on to the snow is 0.94 μg m^{-2} d^{-1} for a dry deposition velocity of 0.01 cm s^{-1} and 2 cm thick fresh snow over Hanle during pre-monsoon season, which is lower compared to the estimated values reported over NCO-P (Yasunari et al., 2010). Thus, the amount of BC accumulated on a snow layer of depth 2 cm during the entire pre-monsoon season is estimated as 21.7 μg kg^{-1} for a mean BC of 109 ± 26 ng m^{-3} in the atmosphere. Using NCO-P measurements during pre-monsoon season, Yasunari et al. (2010) have reported ~ 68 μg kg^{-1} of BC on snow. The major uncertainties in the estimation of BC on snow using the atmospheric BC measurements arise from the lack of accurate information of the dry deposition velocity of BC and physical properties of snow. The dry deposition velocity of the sub-micron aerosols over the snow/ice varies from 0.001 to 1 cm s^{-1} (refer Table S1 of Yasunari et al., 2013) depending on the surface characteristics and turbulence conditions. However, similar to Yasunari et al. (2010), dry deposition velocities used in this study are close to the mean values reported in the literature.

3.2.2. Wet deposition and snowfall events. Wet deposition of BC through below cloud scavenging is the efficient pathway for removing BC from the atmosphere. Despite its importance, it is very difficult to quantify the amount of BC removed from the atmosphere during the precipitation events due to the complex dependence of size and shape of scavenger and BC. Wet deposition of BC aerosols has generally been estimated using bulk models (e.g. Ming et al., 2008) or size segregated numerical models (e.g. Croft et al., 2009). To get a range of BC values on snow due to wet scavenging over the Himalayas, we have estimated scavenging coefficient using: (1) atmospheric BC measurements made during snowfall event; and (2) size-resolved snow scavenging parameterisation. A typical example of BC scavenging due to snowfall events observed over Hanle during summer season (25 August–20 September 2009) (Babu et al., 2011) is shown in Fig. 7a. The snowfall (mm h^{-1}) data are taken from Modern-Era Retrospective Analysis for Research and Applications (MERRA) reanalysis (maintained by NASA Giovanni web portal) as no measurements of snowfall were available at and around Hanle. Simultaneous measurements of relative humidity, temperature and duration of precipitation measured using Automatic Weather Station installed at Hanle are shown in Fig. 7b. It is observed that the relative humidity and precipitation also showed similar variations as that of snowfall from MERRA reanalysis when the observed relative humidity was high and a larger precipitation amount was observed. In general, conspicuous decreases in BC mass concentration have been observed in association with the strong snowfall events. The first snowfall episode lasted for ~ 6 d and during this BC mass concentration decreased from 105 to 7 ng m^{-3}, with a decrease of 16.7 ng m^{-3} d^{-1}. During the second episode, reported on 9–13 September 2009, the BC values again decreased from 40 to 9 ng m^{-3}. From these time series measurements, scavenging coefficient (β) of BC is estimated using the relation

$$\frac{dC_{BC}}{dt} = -\beta C_{BC} \quad (1)$$

where C_{BC} is the BC mass concentration in the atmosphere. Assuming that the decrease in BC measured on 25–31 August over Hanle is solely due to wet scavenging, the estimated value of β for this snowfall event is 0.0065 h^{-1}. The major assumption in this estimation is that the decrease in BC during a snowfall event is completely attributed to snow scavenging.

To further extend this analysis to pre-monsoon season, a size-resolved snow scavenging coefficient (below cloud scavenging) has been estimated from the collision efficiencies for diffusion, interception and impaction processes for

Table 2. The estimated amount BC on snow through dry deposition over Hanle and Satopanth during pre-monsoon season

Station	BC (ng m^{-3})	Dry deposition velocity (cm s^{-1})	Snow density (kg m^{-3})	Snow depth (cm)	Accumulated deposition (μg m^{-2})	BC on snow (μg kg^{-1})
Hanle*	109	0.01	195	2	84.8	21.7
	109	0.054	195	2	457.7	117
	109	0.01	512	2	84.7	8.3
	109	0.01	512	10	84.7	1.7
Satopanth**	190	0.054	195	2	147.7	204.6
	190	0.01	512	10	797.8	2.9

*Climatological mean BC value.
**Measured during September–October 2011.
The dry deposition velocity of BC and snow density are taken from Yasunari et al. (2010), Yasunari et al. (2013).

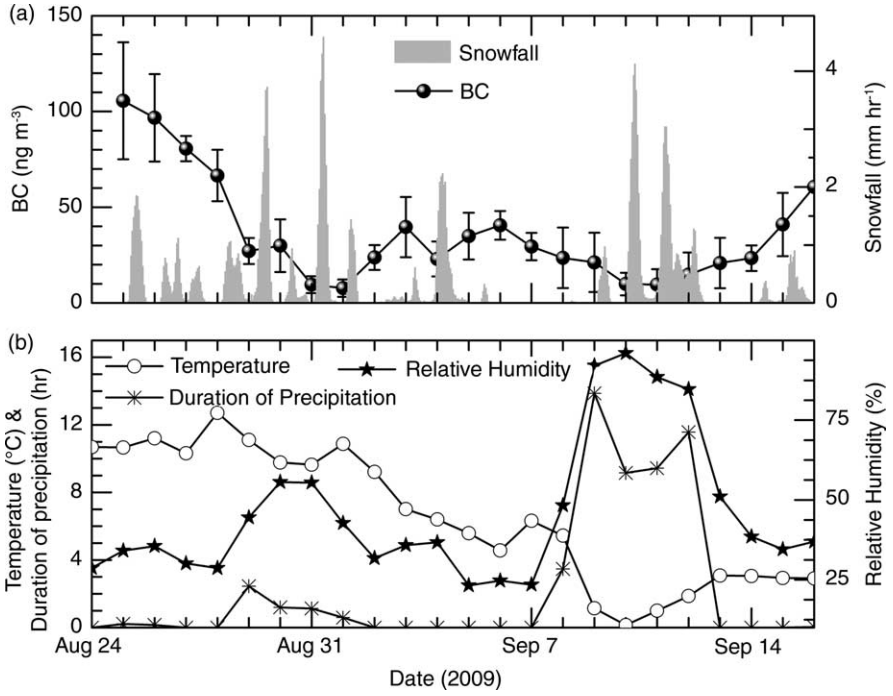

Fig. 7. Temporal variation of aerosols and meteorological parameters during the snowfall event observed at Hanle. The mass concentration of BC in the atmosphere and snowfall data from MERRA reanalysis are shown in (a) and simultaneous measurements of duration of precipitation and relative humidity are shown in (b).

aggregate of planar snow plates as described in the study by Feng (2009).

$$\beta(d_p) = \int_{D_{min}}^{D_{max}} A(V_t - v_t)E(D, d_p)N(D)dD \qquad (2)$$

where D, A, V_t and $N(D)$ represent the diameter, area, terminal velocity and number size distribution of snow particles, respectively. The d_p and v_t represent the diameter and terminal velocity of BC aerosols, respectively. The size-resolved collision efficiency [$E(D, d_p)$], which is a function of D and d_p, for different snowfall rates 0.25, 0.5, 1.0 and 3.0 mm h^{-1} are shown in Fig. 8. Integrating the scavenging coefficients ($\beta(d_p)$) for the BC size distribution (mode radius = 40 nm, sigma = 2.0), the scavenging coefficients are estimated as 0.0044 h^{-1} for the mean snowfall rate of 0.25 mm h^{-1} and 0.0077 h^{-1} for the mean snowfall rate of 0.5 mm h^{-1}. It should be noted that the measurement-based estimate of 0.0065 h^{-1} lies in the above range of β values, close to a snowfall rate of 0.5 mm h^{-1}.

We assume a homogeneous atmosphere of 1000 m in the vertical [$C_{BC} = C_{BC}(z)$ and $\beta = \beta(z)$]. Wet scavenging rate (below cloud) (μg m^{-2} s^{-1}) is estimated as:

$$F_{BC} = \int_{0}^{z=1000m} \beta(z)C_{BC}(z)dh = \beta C_{BC} z \qquad (3)$$

Using the β value estimated from the measurements (0.0065 h^{-1}), the amount of BC scavenged during the first snowfall event (25–31 August) has been estimated as ~6 μg kg^{-1} for a precipitating column of 1000 m and accumulated snow depth of ~9 cm. As there were no direct measurements available on the amount of BC on snow, we could not validate this estimate and this would be attempted in future. The amount of BC aerosols

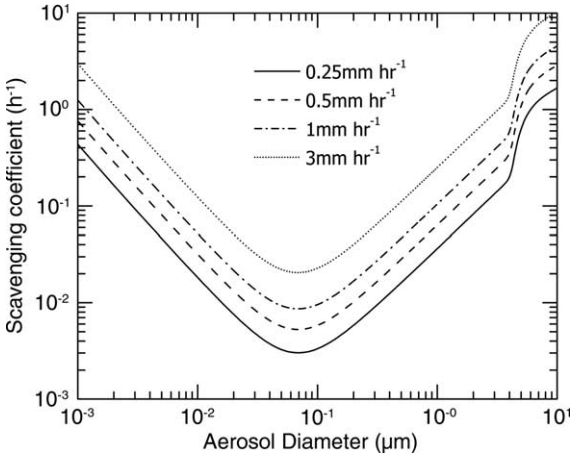

Fig. 8. Size-resolved scavenging coefficients for different snowfall rates estimated using Feng (2009).

deposited on the snow surface during pre-monsoon season via wet scavenging has been estimated based on the modelled mean scavenging efficiency of $0.008\,h^{-1}$ for an accumulated snow depth of 27 cm and an ambient BC mass concentration of 109 ng m^{-3} in the air. The average concentration of BC on snow is estimated to be $29\,\mu g\ kg^{-1}$.

The general empirical relationship connecting the BC on snow and atmosphere is (Davidson et al., 1993),

$$C_{air} = \frac{\rho_{air} C_{snow}}{\omega} \quad (4)$$

where C_{air} and C_{snow} are the mass concentration of BC in the atmosphere and snow, respectively, ρ_{air} is the air density, which is calculated for the mean altitude of the Himalayas (5 km) using mean pressure and temperature and ω is the scavenging ratio. The global average value of ω ($=125$) reported by Jacobson (2004) is adopted for this study. The mean BC concentration in the snow for the pre-monsoon season is thus estimated as $19.5\,\mu g\ kg^{-1}$. Even though snowfall events are less frequent over Hanle, it occurs in the adjacent areas. Based on the monthly mean snowfall data from MERRA reanalysis, it is found that winter snowfall continues till May over the Western Himalayas, which could lead to the increase in snow scavenging of BC due to the increase in atmospheric BC during pre-monsoon and decreases the BC loading in snow due to the dilution effects in the larger snow column. Jacobson (2004) has estimated global averaged BC concentration in snow and sea ice as $5\,\mu g\ kg^{-1}$, out of which almost 98% comes from precipitation scavenging.

3.3. Radiative impacts of BC over the Himalayas

3.3.1. Direct radiative forcing. Based on the extensive measurements of aerosol properties from Hanle and NCO-P, clear sky DRFs due to aerosols were estimated for different surface albedo conditions during pre-monsoon and winter season. The general characteristics of physical, chemical and optical properties of Himalayan aerosols and the transport pathways over Hanle and NCO-P have been extensively discussed (Pant et al., 2006; Bonasoni et al., 2010; Gobbi et al., 2010; Marcq et al., 2010; Marinoni et al., 2010; Moorthy et al., 2010; Verma et al., 2010; Babu et al., 2011; Sharma et al., 2012) and hence not repeated here. Table 3 depicts the mean values of aerosol optical depth (AOD), single scattering albedo (SSA) and BC mass concentration in the atmosphere over the Himalayan stations as well as at the lower Himalayan stations during pre-monsoon and winter seasons. In general, AOD over Hanle and NCO-P are lower than those reported for the other stations (Pant et al., 2006). The aerosols over NCO-P are more absorbing compared to those over Hanle and the low SSA over NCO-P persists throughout the year (Gobbi et al., 2010; Marcq et al., 2010). The columnar SSA retrieved from the CIMEL radiometer measurements and in situ measurements of scattering and absorption coefficients also indicate low SSA over the NCO-P, which indicates significant contribution of anthropogenic absorbing aerosols over Khumbu valley compared to western trans-Himalayas (Gobbi et al., 2010; Marcq et al., 2010; Lu et al., 2012). Verma et al. (2010) have reported an annual mean AOD of 0.05 ± 0.001 and SSA of 0.96 using sun/sky radiometer measurements at Hanle. Based on the aerosol optical properties measured at Hanle and NCO-P, short-wave solar flux (0.25–4.0 μm) reaching at the TOA and surface were estimated for conditions with and without aerosols using the Santa Barbara DISORT model (SBDART, Ricchiazzi et al., 1998) for two surface albedo conditions: (1) snow and (2) sand. We have used the standard (default) vertical profiles of aerosols used in the SBDART model. It assumes that extinction profiles follow an exponential decrease with a scale height of 1.5 km and SSA and phase function remains independent of altitude. The measured values of columnar water vapour content and ozone were also fed into the model for a more accurate estimation of the solar flux (Gobbi et al., 2010). Several studies have shown that the modelled solar flux matches well with the measured flux using pyranometer (Babu et al., 2012). The difference in the flux at TOA (surface) in the presence of aerosols (F_{aero}) compared to no-aerosol ($F_{no\text{-}aero}$) condition is integrated over the entire zenith angle (time) to obtain the

Table 3. Optical properties of aerosols over Hanle, NCO-P and lower Himalayan stations (Nainital, Dehradun, and Kullu) during pre-monsoon (March–May) and winter (December–February) seasons

Station	Season	AOD	SSA	BC (ng m^{-3})
Hanle	Pre-monsoon	0.063 ± 0.002[a]	0.97[a]	109 ± 27[b]
	Winter	0.040 ± 0.001[a]	0.96[a]	67 ± 28[b]
NCO-P	Pre-monsoon	0.050 ± 0.004[c]	0.844[d]	320 ± 469[e]
	Winter	0.045 ± 0.004[c]	0.869[d]	125 ± 147[e]
Nainital	Pre-monsoon	0.21 ± 0.08[b]	NA	1340 ± 50[b]
	Winter	0.09 ± 0.09[b]	0.9[f]	1100 ± 60[b]
Kullu	Pre-monsoon	0.41 ± 0.14[b]	NA	6922[b]
	Winter	0.27 ± 0.15[b]	NA	3730[b]
Dehradun	Pre-monsoon	0.25 ± 0.10[b]	NA	6646 ± 492[b]
	Winter	0.24 ± 0.07[b]	NA	4282 ± 606[b]

[a]Verma et al. (2010); [b]Present study; [c]Gobbi et al. (2010); [d]Marcq et al. (2010); [e]Marinoni et al. (2010); [f]Pant et al. (2006).
NA, not available.

diurnally averaged clear sky aerosol radiative forcing (Moorthy et al., 2009).

$$\mathrm{DRF} = \frac{\int_0^{24} (F_{\mathrm{no-aero}} - F_{\mathrm{aero}})dh}{\int_0^{24} dh} \quad (5)$$

where dh is the time in hours.

The aerosol DRF at the TOA for pre-monsoon and winter seasons over Hanle and NCO-P is shown in Fig. 9a. It should be noted that aerosol forcing at TOA is highly positive (warming) over a snow surface (high albedo), whereas for the sandy surfaces the TOA forcing over Hanle becomes negative, though it still remains weakly positive over NCO-P. This discrepancy between the forcing values over the Hanle and NCO-P arises mainly because of the low SSA (0.89) values over NCO-P compared to Hanle (0.96). Marcq et al. (2010) have reported that the local radiative forcing of background aerosols (AOD at 550 nm = 0.01) over NCO-P during pre-monsoon season is 2.1 W m^{-2} above the snow surface and 0.2 W m^{-2} over the rocky surfaces. These analyses clearly depict that the same aerosol system induces distinctly different radiative effects at the TOA depending on the surface albedo. Hence, the accurate characterisation of absorbing aerosols and spectral surface albedo is essential in understanding the regional heterogeneity of aerosol DRFs at TOA. As the annual mean snow cover accounts for only 18% of the total geographical area of the Himalayas (Gurung et al., 2011), the large heterogeneities in the surface albedos are very important in the estimation of regional climate forcings. A precise analysis of snow cover seasonality is also essential for a better understanding of the DRF over the Himalayan region.

3.3.2. Snow albedo radiative forcing. Radiative implications of snow darkening due to BC deposition are investigated using the spectral albedo simulated by the two stream, multi-layer Snow, Ice, and Aerosol Radiation (SNICAR,

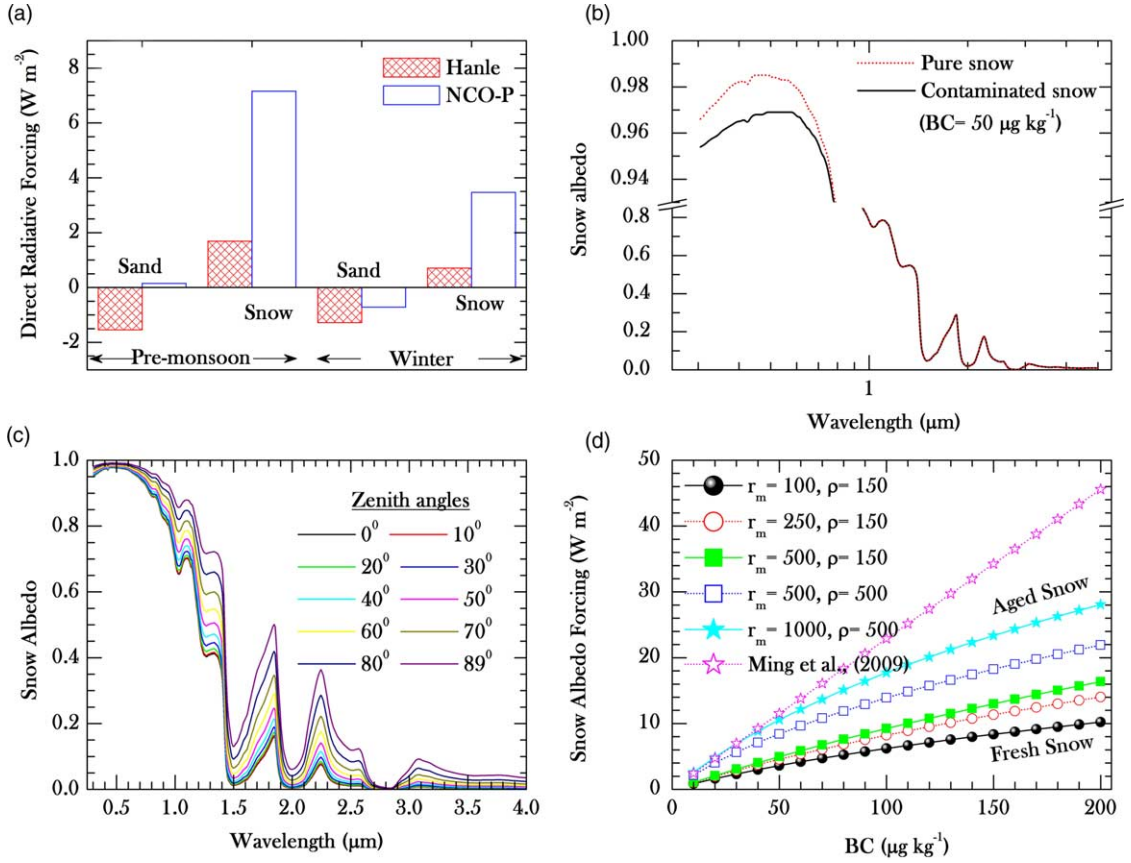

Fig. 9. (a) Direct radiative forcing due to composite aerosols on snow and sandy surfaces over Hanle and NCO-P during pre-monsoon season; (b) spectral variation of snow albedo for pure and contaminated snow (BC loading of 50 μg kg^{-1}) simulated using SNICAR model; (c) spectral variations of pure snow albedo for different zenith angle conditions; (d) variation of snow-albedo radiative forcing (SARF) as a function of BC concentration in snow for different micro-physical conditions of snow. The estimated BC values in snow for dry deposition range from 1 to 117 μg kg^{-1} and wet deposition accounts for 29 μg kg^{-1} for BC in snow.

Flanner et al., 2007) model for different combinations of effective radius of snow grain, snow density and snow pack thickness and using a radiative transfer model (SBDART) for simulating the fluxes reaching the TOA and surface for pure and contaminated snow-albedo conditions. The spectral albedo of fresh and contaminated snow is estimated using the SNICAR model for mid-latitude winter atmospheric conditions with various snow density values ranging from 195 to 512 kg m^{-3} (taken from Yasunari et al., 2010) and snowfall rate and snow depth from MERRA reanalysis data. A sensitivity analysis has been carried out to investigate the decrease in snow albedo and its radiative forcing for a range of 10– 200 μg kg^{-1} of BC loading in snow. The values of BC on snow considered in this study are close to the earlier assessments made by Ming et al. (2008), Xu et al. (2009) and Kaspari et al. (2011) over the northern slopes of the Himalayas.

Figure 9b depicts the spectral albedo of pure and contaminated (BC loading of 50 μg kg^{-1}) snow simulated using SNICAR model for a typical snow grain radius of 150 μm (Aoki et al., 2000), snow density of 200 kg m^{-3} and snow pack thickness of 2 cm. It is reported that BC aerosols significantly reduce the snow albedo more in the visible wavelengths compared to near-infrared wavelengths (Warren and Wiscombe, 1980). Radiative forcings due to snow darkening have then been estimated using the short-wave fluxes simulated by SBDART model for the wavelength range of 0.25–4.0 μm using the surface albedo of pure and contaminated snow (shown in Fig. 9b) estimated using SNICAR model. The difference between the shortwave (0.25–4.0 μm) fluxes at the TOA for the simulations with pure and dirty snow albedo is defined as the snow-albedo radiative forcing (SARF). As the snow albedo is strongly dependent on the solar zenith angle especially in the near-infrared wavelengths (as shown in Fig. 9c) (Wiscombe and Warren, 1980), the radiative transfer simulations were carried out for the entire zenith angles to calculate the diurnally averaged radiative forcing at the TOA. Fig. 9d depicts the variation of SARF with BC loading varying from 10 to 200 μg kg^{-1} for different microphysical conditions of snow (representing fresh and aged snow) during pre-monsoon season. Using the functional dependence of BC on snow reported by Ming et al. (2009) for various glaciers over southern and northern slopes of the Himalayas, we have estimated the surface albedo reduction ($\Delta\alpha(\%) = 0.0757*BC + 0.0575$) for various BC loading values and the corresponding SARF is also shown in Fig. 9d. For the range of 10–200 μg kg^{-1} of BC in snow, the diurnally averaged forcing due to snow darkening has been found to vary from 0.87 to 10.2 W m^{-2} for fresh snow and from 2.6 to 28.1 W m^{-2} for the aged snow.

Based on the atmospheric BC measurements at NCO-P, Yasunari et al. (2010) have reported an albedo reduction of 2.0–5.2% for a BC concentration of 26–68.2 μg kg^{-1} on snow following the methodology of Ming et al. (2009). Our study shows that the BC mass concentration on snow reduces the surface albedo by 1.5–4.6% over the southern slopes of western trans-Himalayas, the difference being primarily attributed to the lower BC concentration in the atmosphere at Hanle compared with Khumbu valley. These values would vary significantly with the snow ageing and it is very important to know the micro-physical properties of snow while assessing the impacts of BC on snow albedo. Even though the DRFs of composite aerosols were much lower than the snow-albedo forcing, it reinforces the warming at the TOA. Whereas over thin snow layers, where critical SSA is much lower than the aerosol SSA, cooling of TOA due to aerosol direct forcing partially compensates the SARF. It should be kept in mind that the range of atmospheric BC values used in this study is highly weighted by the Hanle measurements, which is quite far from the major glaciers. In this study, we have assumed several physical properties of snow to estimate the SARF, which need to be verified in future. Forthcoming campaigns under the ARFI project would focus mainly on these gap areas, to gain a better picture of radiative implications of BC aerosols on Himalayan glacier melting.

4. Conclusions

Continuous measurements of BC aerosols carried out at distinct geographical locations over the western trans-Himalayas (Hanle, Satopanth), central Himalayas (NCO-P) and lower Himalayan regions (Dehradun, Kullu, Nainital) indicate significant BC concentration in the atmosphere during the pre-monsoon period. The measurements of BC concentrations from Hanle and NCO-P showed strong seasonal variations with pre-monsoon high and summer minimum. An expedition to Satopanth Glaciers revealed high BC concentration in the atmosphere even during the summer season in association with local activities with values comparable to pre-monsoon values at Hanle. Based on the measurements of atmospheric BC made at Hanle, dry deposition and wet deposition flux of BC aerosols on the snow surface is estimated. It is found that the range of BC values expected on snow due to dry deposition in the western trans-Himalayas would be 1.7–117 μg kg^{-1} during the pre-monsoon season. The optical properties of aerosols measured over Hanle during pre-monsoon season are used to further understand the range of clear sky DRF values at TOA for different surface albedo conditions. The estimated DRF over a snow surface is $+1.69$ W m^{-2} compared to -1.54 W m^{-2} over a sandy surface. The snow-albedo forcing estimated for the range of BC in snow (10–200 μg kg^{-1}) varied from 0.87 to 10.2 W m^{-2} for fresh snow and from 2.6 to 28.1 W m^{-2}

for aged snow. Over snow-covered regions, both DRF due to atmospheric aerosols and snow-albedo forcing due to BC tend to warm the TOA during pre-monsoon, while former heat the atmosphere and latter warm the surface, in turn adding more energy to the Earth–Atmosphere system and thus amplifying the snow-albedo feedback mechanism.

5. Acknowledgments

The work was carried out under the ARFI project of Geosphere Biosphere Program of Indian Space Research Organisation. The authors are grateful to the investigators, Yogesh Kant (IIRS Dehradun), J. C. Kuniyal (GBPIHED, Mohal-Kullu) and P. Pant (Aries, Nainital) for supporting the measurements. One of the authors (V. S. Nair) greatly acknowledges Prof. Mark Flanner, University of Michigan, USA for providing the SNICAR model and valuable suggestions that improved the analyses presented in this article. The authors thank Dr. Kimothi and other colleagues of Uttarakhand Space Application Centre for supporting the expedition to Satopanth glaciers. MERRA data used in this study have been provided by the Global Modeling and Assimilation Office (GMAO) at NASA Goddard Space Flight Center through the NASA GES DISC online archive. We thank the anonymous reviewers for their useful comments and suggestions to improve the quality of the manuscript.

References

Aoki, T., Aoki, T., Fukabori, M., Hachikubo, A., Tachibana, Y. and co-authors. 2000. Effects of snow physical parameters on spectral albedo and bidirectional reflectance of snow surface. *J. Geophys. Res.* **105**, 10219–10236.

Arnott, W. P., Hamasha, K., Moosmueller, H., Sheridan, P. J. and Ogren, J. A. 2005. Towards aerosol light absorption measurements with a 7-wavelength aethalometer: evaluation with a photoacoustic instrument and a 3 wavelength nephelometer. *Aerosol. Sci. Technol.* **39**, 17–29.

Babu, S. S., Chaubey, J. P., Moorthy, K. K., Gogoi, M. M., Kompalli, S. K. and co-authors. 2011. High-altitude (4520 m amsl) measurements of black carbon aerosols over western trans-Himalayas: seasonal heterogeneity and source apportionment. *J. Geophys. Res.* **116**, D24201.

Babu, S. S., Gogoi, M. M., Kumar, V. H. A., Nair, V. S. and Moorthy, K. K. 2012. Radiative properties of Bay-of-Bengal aerosols: spatial distinctiveness and source impacts. *J. Geophys. Res.* **117**, D06213.

Babu, S. S., Moorthy, K. K. and Satheesh, S. K. 2004. Aerosol black carbon over Arabian Sea during inter monsoon and summer monsoon seasons. *Geophys. Res. Lett.* **31**, L06104.

Bolch, T., Kulkarni, A., Kaab, A., Huggel, C., Paul, F. and co-authors. 2012. The state and fate of Himalayan glaciers. *Science*. **336**, 6079.

Bonasoni, P., Laj, P., Marinoni, A., Sprenger, M., Angelini, F. and co-authors. 2010. Atmospheric brown clouds in the Himalayas: first two years of continuous observations at the Nepal Climate Observatory-Pyramid (5079 m). *Atmos. Chem. Phys.* **10**, 7515–7531.

Croft, B., Lohmann, U., Martin, R. V., Stier, P., Wurzler, S. and co-authors. 2009. Aerosol size-dependent below-cloud scavenging by rain and snow in the ECHAM5-HAM. *Atmos. Chem. Phys.* **9**, 4653–4675.

Davidson, C. I., Jaffrezo, J. L., Mosher, B. W., Dibb, J. E., Borys, R. D. and co-authors. 1993. Chemical constituents in the air and snow at Dye 3, Greenland: II. Analysis of episodes in April 1989. *Atmos. Environ.* **27**(A), 2723–2738.

Feng, J. 2009. A size-resolved model for below-cloud scavenging of aerosols by snowfall. *J. Geophys. Res.* **114**, D08203.

Flanner, M. G., Zender, C. S., Hess, P. G., Mahowald, N. M., Painter, T. H. and co-authors. 2009. Springtime warming and reduced snow cover from carbonaceous particles. *Atmos. Chem. Phys.* **9**, 2481–2497.

Flanner, M. G., Zender, C. S., Randerson, J. T. and Rasch, P. J. 2007. Present-day climate forcing and response from black carbon in snow. *J. Geophys. Res.* **112**, D11202.

Ganguly, D., Ginoux, P., Ramaswamy, V., Dubovik, O., Welton, J. and co-authors. 2009. Inferring the composition and concentration of aerosols by combining AERONET and MPLNET data: comparison with other measurements and utilization to evaluate GCM output. *J. Geophys. Res.* **114**, D16203.

Gobbi, G. P., Angelini, F., Bonasoni, P., Verza, G. P., Marinoni, A. and co-authors. 2010. Sunphotometry of the 2006–2007 aerosol optical/radiative properties at the Himalayan Nepal Climate Observatory-Pyramid (5079 m a.s.s.). *Atmos. Chem. Phys.* **10**, 11209–11221.

Gurung, D. R., Kulkarni, A. V., Giriraj, A., Aung, K. S., Shrestha, B. and co-authors. 2011. Changes in seasonal snow cover in Hindu Kush-Himalayan region. *Cryosphere. Discuss.* **5**, 755–777.

Hahn, D. G. and Manabe, S. 1975. The role of mountains in the south Asian monsoon circulation. *J. Atmos. Sci.* **32**, 1515–1541.

Hansen, A. D. A., Rosen, H. and Novakov, T. 1984. The Aethalometer, an instrument for the real-time measurement of optical absorption by aerosol particles. *Sci. Total. Environ.* **36**, 191–196.

Hansen, J. and Nazarenko, L. 2004. Soot climate forcing via snow and ice albedos. *Proc. Natl. Acad. Sci. U. S. A.* **101**(2), 423–428.

Hansen, J., Sato, M. and Ruedy, R. 1997. Radiative forcing and climate response. *J. Geophys. Res.* **102**, 6831–6864.

Hansen, J., Sato, M., Ruedy, R., Nazarenko, L., Lacis, A. and co-authors. 2005. Efficacy of climate forcings. *J. Geophys. Res.* **110**, D18104.

Huang, J., Fu, Q., Zhang, W., Wang, X., Zhang, R. and co-authors. 2011. Dust and black carbon in seasonal snow across northern China. *Bull. Am. Meteorol. Soc.* **92**, 175–181.

IPCC. 2007. The scientific basis. *Contribution of Working Group I to the Fourth Assessment Report of the Intergovernmental Panel on Climate Change*. Cambridge University Press, New York.

Jacobson, M. Z. 2004. Climate response of fossil fuel and biofuel soot, accounting for soots feedback to snow and sea ice albedo and emissivity. *J. Geophys. Res.* **109**, D21201.

Kaspari, S. D., Schwikowski, M., Gysel, M., Flanner, M. G., Kang, S. and co-authors. 2011. Recent increase in black carbon concentrations from a Mt. Everest ice core spanning 1860–2000 AD. *Geophys. Res. Lett.* **38**, L04703.

Kopacz, M., Mauzerall, D. L., Wang, J., Leibensperger, E. M., Henze, D. K. and co-authors. 2011. Origin and radiative forcing of black carbon transported to the Himalayas and Tibetan Plateau. *Atmos. Chem. Phys.* **11**, 2837–2852.

Lau, K. M., Kim, M. K. and Kim, K. M. 2006. Asian summer monsoon anomalies induced by aerosol direct forcing: the role of the Tibetan Plateau. *Clim. Dyn.* **26**, 855–864.

Lu, Z., Streets, D. G., Zhang, Q. and Wang, S. 2012. A novel back-trajectory analysis of the origin of black carbon transported to the Himalayas and Tibetan Plateau during 1996–2010. *Geophys. Res. Lett.* **39**, L01809.

Marcq, S., Laj, P., Roger, J. C., Villani, P., Sellegri, K. and co-authors. 2010. Aerosol optical properties and radiative forcing in the high Himalayas based on measurements at the Nepal Climate Observatory-Pyramid site (5079 m a.s.l.). *Atmos. Chem. Phys.* **10**, 5859–5872.

Marinoni, A., Cristofanelli, P., Laj, P., Duchi, R., Calzolari, F. and co-authors. 2010. Aerosol mass and black carbon concentrations, a two year record at NCO-P (5079 m, Southern Himalayas). *Atmos. Chem. Phys.* **10**, 8551–8562.

Menon, S., Koch, D., Beig, G., Sahu, S., Fasullo, J. and co-authors. 2010. Black carbon aerosols and the third polar ice cap. *Atmos. Chem. Phys.* **10**, 4559–4571.

Ming, J., Cachier, H., Xiao, C., Qin, D., Kang, S. and co-authors. 2008. Black carbon record based on a shallow Himalayan ice core and its climatic implications. *Atmos. Chem. Phys.* **8**, 1343–1352.

Ming, J., Du, Z., Xiao, C., Xu, X. and Zhang, D. 2012. Darkening of the mid-Himalayas glaciers since 2000 and the potential causes. *Environ. Res. Lett.* **7**, 014021.

Ming, J., Xiao, C., Cachier, H., Qin, D., Qin, X. and co-authors. 2009. Black carbon (BC) in the snow of glaciers in west China and its potential effects on albedos. *Atmos. Res.* **92**, 114–123.

Ming, J., Xiao, C., Sun, J., Kang, S. and Bonasoni, P. 2010. Carbonaceous particles in the atmosphere and precipitation of the Namco region, central Tibet. *J. Environ. Sci.* **22**(11), 1748–1756.

Moorthy, K. K., Babu, S. S., Manoj, M. R. and Satheesh, S. K. 2013. Buildup of aerosols over the Indian region. *Geophys. Res. Lett.* **40**, 1011.

Moorthy, K. K., Beegum, S. N., Babu, S. S., Smirnov, A., John, S. R. and co-authors. 2010. Optical and physical characteristics of Bay of Bengal aerosols during WICARB: spatial and vertical heterogeneities in the marine atmospheric boundary layer and in the vertical column. *J. Geophys. Res.* **115**, D24213.

Moorthy, K. K., Nair, V. S., Babu, S. S. and Satheesh, S. K. 2009. Spatial and vertical heterogeneities of aerosol radiative forcing over the oceanic regions surrounding the Indian peninsula: climate implications. *Q. J. Roy. Meteorol. Soc.* **135**, 2131–2145.

Müller, T., Henzing, J. S., de Leeuw, G., Wiedensohler, A., Alastuey, A. and co-authors. 2011. Characterization and intercomparison of aerosol absorption photometers: result of two intercomparison workshops. *Atmos. Meas. Tech.* **4**, 245–268.

Nair, V. S., Babu, S. S. and Moorthy, K. K. 2008. Spatial distribution and spectral characteristics of aerosol single scattering albedo over the Bay of Bengal inferred from shipborne measurements. *Geophys. Res. Lett.* **35**, L10806.

Nair, V. S., Moorthy, K. K., Alappattu, D. P., Kunhikrishnan, P. K., George, S. and co-authors. 2007. Wintertime aerosol characteristics over the Indo-Gangetic Plain (IGP): impacts of local boundary layer processes and long-range transport. *J. Geophys. Res.* **112**, D13205.

Nair, V. S., Solmon, F., Giorgi, F., Mariotti, L., Babu, S. S. and co-authors. 2012. Simulation of South Asian aerosols for regional climate studies. *J. Geophys. Res.* **117**, D04209.

Nigam, S. and Bollasina, M. 2010. The 'elevated heat pump' hypothesis for the aerosol-monsoon hydroclimate link: "grounded" in observations? *J. Geophys. Res.* **115**, D16201.

Painter, T. H., Barrett, A. P., Landry, C. C., Neff, J. C., Cassidy, M. P. and co-authors. 2007. Impact of disturbed desert soils on duration of mountain snow cover. *Geophys. Res. Lett.* **34**, L12502.

Pant, P., Hegde, P., Dumka, U. C., Sagar, R., Satheesh, S. K. and co-authors. 2006. Aerosol characteristics at a high-altitude location in central Himalayas: optical properties and radiative forcing. *J. Geophys. Res.* **111**, D17206.

Petzold, A. and Schonlinner, M. 2004. Multi-angle absorption photometry. A new method for the measurement of aerosol light absorption and atmospheric black carbon. *J. Aerosol. Sci.* **35**, 421–441.

Qian, Y., Flanner, M. G., Leung, L. R. and Wang, W. 2011. Sensitivity studies on the impacts of Tibetan Plateau snowpack pollution on the Asian hydrological cycle and monsoon climate. *Atmos. Chem. Phys.* **11**, 1929–1948.

Ramanathan, V. and Carmichael, G. 2008. Global and regional climate changes due to black carbon. *Nat. Geosci.* **1**, 221–227.

Ricchiazzi, P., Yang, S., Gautier, C. and Sowle, D. 1998. SBDART: a research and teaching software tool for plane-parallel radiative transfer in the earth's atmosphere. *Bull. Am. Meteorol. Soc.* **79**(10), 2101–2114.

Sharma, N. L., Kuniyal, J. C., Singh, M., Dhyani, P. P., Mathela, C. S. and co-authors. 2012. Three years aerosol meteorology derived from ground based sun radiometry over Mohal in the Kullu valley of Northwest Himalayan region, India. *J. Atmos. Sol. Terr. Phys.* **77**, 26–39.

Shindell, D., Schulz, M., Ming, Y., Takemura, T., Faluvegi, G. and co-authors. 2010. Spatial scales of climate response to inhomogeneous radiative forcing. *J. Geophys. Res.* **115**, D19110.

Vaux, H. J., Jr., Balk, D., Cook, E. R., Gleick, P., Lau, W. K.-M. and co-authors. 2012. *Himalayan Glaciers: Climate Change, Water Resources, and Water Security*. National Academies Press, Washington, DC.

Verma, N., Bagare, S. P., Ningombam, S. S. and Singh, R. B. 2010. Aerosol optical properties retrieved using skyradiometer at Hanle in western Himalayas. *J. Atmos. Sol. Terr. Phys.* **72**, 115–124.

Warren, S. G. and Wiscombe, W. J. 1980. A model for the spectral albedo of snow. II: snow containing atmospheric aerosols. *J. Atmos. Sci.* **37**, 2734–2745.

Wiscombe, W. J. and Warren, S. G. 1980. A model for the spectral albedo of snow. I: pure snow. *J. Atmos. Sci.* **37**, 2712–2733.

Xu, B., Cao, J., Hansen, J., Yao, T., Joswia, D. J. and co-authors. 2009. Black soot and the survival of Tibetan glaciers. *Proc. Natl. Acad. Sci. U. S. A.* **106**, 22114–22118.

Yasunari, T. J., Bonasoni, P., Laj, P., Fujita, K., Vuillermoz, E. and co-authors. 2010. Estimated impact of black carbon deposition during premonsoon season from Nepal Climate Observatory Pyramid data and snow albedo changes over Himalayan glaciers. *Atmos. Chem. Phys.* **10**, 6603–6615.

Yasunari, T. J., Tan, Q., Lau, K.-M., Bonasoni, P., Marinoni, A. and co-authors. 2013. Estimated range of black carbon dry deposition and the related snow albedo reduction over Himalayan glaciers during dry pre-monsoon periods. *Atmos. Environ.* **78**, 259–267.